Reactions of NH_2 Species with Hydrogen and NO on the Pt(100)-(1×1) Surface

M. Yu. Smirnov* and D. Zemlyanov†

Boreskov Institute of Catalysis, Prosp. Akademika Lavrentieva 5, Novosibirsk 630090, Russian Federation

Received: October 31, 1999; In Final Form: March 7, 2000

The formation of the $NH_{2,ads}$ amino species and its further reactions with hydrogen and NO on the unreconstructed Pt(100) surface were studied by means of high-resolution electron energy loss spectroscopy (HREELS) and temperature-programmed reaction (TPR) spectroscopy. The $NH_{2,ads}$ amino species forms during the reaction between H_{ads} and NO at 300 K. $NH_{2,ads}$ can be oxidized by NO at a temperature higher than 260 K. The reaction at $T \geq 300$ K results in the evolution of N_2 and water. An essential amount of N_{ads} accumulates on the surface after the reaction at ~260 K and desorbs as a low-temperature TPR peak of N_2 at 320 K. TPR in a saturated coadsorption layer of NO_{ads} and $NH_{2,ads}$ prepared at 100 K shows an "explosive" behavior, manifesting itself in the evolution of narrow TPR peaks of N_2 and H_2O at ~370 K. TPR in an unsaturated coadsorption layer of NO_{ads} and $NH_{2,ads}$ proceeds at a much lower temperature of <300 K, resulting in the "nonexplosive" desorption peaks of N_2 and H_2O. The reaction between the $NH_{2,ads}$ and H_{ads} species in the temperature range of 350−470 K results in ammonia evolution. At $T < 400$ K, NH_3 forms through the addition of a hydrogen atom to $NH_{2,ads}$ and competes with the H_{ads} recombination. At higher temperature, >400 K, the dissociation of $NH_{2,ads}$ serves as a source of hydrogen atoms for the $NH_{2,ads}$ hydrogenation, leading to the parallel evolution of ammonia along with N_2 and H_2. The mechanism of the formation of $NH_{2,ads}$ species and its further reactions with NO and hydrogen on the Pt(100)-(1×1) surface are discussed in detail.

1. Introduction

The reaction between NO and H_2 on platinum-based catalysts is of great interest due to its practical importance.[1−3] The selectivity to N_2, N_2O, and NH_3 as reaction products depends strongly on the reaction conditions as well as on the catalyst structure. Since imido NH and amino NH_2 species are supposed to play a role of intermediates for the ammonia synthesis, these species have become a subject of numerous studies.[4−14] The NH_{ads} and $NH_{2,ads}$ species were found in the course of the hydrogenation of atomic nitrogen on Rh(100),[4,5] Rh(111),[6] Pd-(100),[4,5,7] Ru(0001),[8,9] Ru(10$\bar{1}$0),[10] Ni(110),[11] and RhPt-(100).[4,5,12] The distribution between $NH_{x,ads}$ species and their configuration depends strongly on the nature of the metal surface and reaction conditions. Both the NH_{ads} and $NH_{2,ads}$ species were observed on the Pt(100) surface during the reaction between NO and H_2.[13,14] The significant decrease of a work function observed during the oscillatory and steady-state regimes of the NO + H_2 reaction on Pt(100) was assigned to the formation of ammonia $NH_{3,ads}$.[15] However, one cannot rule out the formation of the NH_{ads} and/or $NH_{2,ads}$ species because they are expected to cause a decrease of the work function as well. The theoretical simulations show that including the $NH_{x,ads}$ species into a scheme of the NO + H_2 reaction is necessary for a proper modeling of the reaction kinetic and a branch ratio of the products.[16−18]

In our previous paper,[14] we have reported a detailed analysis of the vibrational data relevant to the $NH_{2,ads}$ species, which forms during the titration of H_{ads} by NO on the unreconstructed Pt(100)-(1×1) surface at 300 K. The $NH_{2,ads}$ species occupies a bridge position bonding via a nitrogen atom to two surface platinum atoms. The molecular plane of the species is approximately normal with respect to the surface.[14] In the present work we aimed to study the reactions of the $NH_{2,ads}$ species with H_2 and NO in order to understand its role in the mechanism of the NO + H_2 reaction on the unreconstructed Pt(100)-(1×1) surface.

2. Experimental Section

The experiments were performed in a stainless steel chamber of a VG ADES 400 electron spectrometer (base pressure ≤ 5 × 10^{-11} mbar). High-resolution electron energy loss (HREEL) spectra were obtained in the specular direction at an angle of approximately 35° with respect to the surface normal, using an EMU 50 monochromatic electron gun and a 150° hemispheric deflector type electron energy analyzer. The HREELS resolution, measured as full width at the half-maximum (fwhm) of the elastic peak, was approximately 80 cm^{-1} (10 meV) with a kinetic energy of electrons of approximately 2.5 eV. Temperature-programmed reaction (TPR) spectra were obtained at a heating rate of 10 K/s by means of a VG QXK 400 quadrupole mass-spectrometer supplied with a twin cathode assembly and a channeltron detector. A self-designed processor-controlled device was interfaced to the spectrometer for the acquisition of the HREELS and mass spectrometer data and for controlling temperature.[19,20]

A Pt single crystal oriented along the (100) direction within <0.5° was used in the experiments. The sample, spot-welded between two tantalum wires, could be heated resistively to 1200 K. The temperature of the crystal was measured by means of a chromel−alumel thermocouple spot-welded to an edge of the crystal. The cleaning procedure of the Pt(100) surface included Ar^+-etching and annealing cycles in oxygen and in a vacuum. The clean and well-annealed Pt(100) surface showed a (5 × 20) LEED (low-energy electron diffraction) pattern corresponding to the hexagonal structure of the surface. The procedures

* Corresponding author. E-mail: smirnov@catalysis.nsk.su.
† Present address: Worcester Polytechnic Institute, 100 Institute Rd., Worcester, MA 10609. E-mail: dzem@wpi.edu.

10.1021/jp993863r CCC: $19.00
Published on Web 04/22/2000

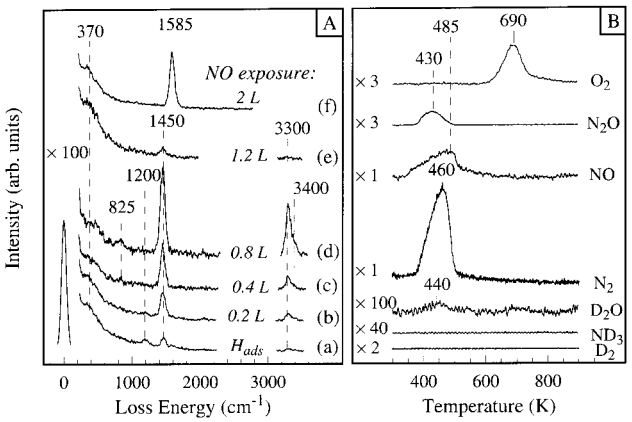

Figure 1. (A) Titration of the saturated hydrogen adsorption layer on the Pt(100)-(1×1) surface with NO at 300 K. HREELS spectra taken from (a) the saturated H_{ads} layer and after subsequent exposure to (b) 0.2, (c) 0.4, (d) 0.8, (e) 1.2, and (f) 2 langmuirs of NO. (B) TPR spectra of D_2, D_2O, $^{15}ND_3$, $^{15}N_2$, ^{15}NO, O_2, and $^{15}N_2O$ taken after exposure of the saturated D_{ads} layer to 3 langmuirs of ^{15}NO at 300 K.

of preparation of the unreconstructed (1×1) surface can be found elsewhere.[21] D_2 and ^{15}NO were used for the TPR experiments in order to increase the reliability of the identification of the products by mass spectrometry. The exposure was measured in langmuirs; 1 langmuir ≡ 1.33×10^{-6} mbar·s. The coverage was measured in monolayers; 1 monolayer is equal to the number of platinum atoms in the topmost layer of the unreconstructed (1×1) surface, i.e., 1.28×10^{15} cm^{-2}.

3. Results

3.1. Formation of $NH_{2,ads}$ and Its Further Reaction with NO. HREEL spectra shown in Figure 1A were taken after an exposure of the H_{ads} layer on the Pt(100)-(1×1) surface to NO at 300 K. The original H_{ads} layer on the Pt(100)-(1×1) surface was prepared as follows:

- The Pt(100)-(hex) surface was exposed to NO at 300 K up to saturation in order to lift the (hex) surface reconstruction.[22,23]
- The NO_{ads} layer was heated at 420 K for 1 min. Heating induces NO_{ads} desorption, producing vacant sites inside the originally dense NO_{ads}/(1×1) islands. The vacant sites are necessary for the activation of the following titration of NO_{ads} by hydrogen.[13,24,25]
- The as-activated NO_{ads} layer was exposed to 25 langmuir of H_2 at 300 K in order to remove NO_{ads} and O_{ads} and to form a H_{ads} layer on the Pt(100)-(1×1) surface.[13,24,25]

The as-prepared H_{ads} layer contains two states of H_{ads}[21] with a total coverage of 0.6 monolayer.[26] A 2-fold bridge state results in a band at 1200 cm^{-1} (spectrum a of Figure 1A), whereas a major state, occupying a 4-fold hollow position, does not show any bands in the specular direction.[21] The presence of the $NH_{2,ads}$ species in the amount of 0.01 monolayer manifests itself in the appearance of weak bands at 1450 and 3300 cm^{-1} due to the $\delta(NH_2)$ scissors and $\nu_s(NH_2)$ symmetric stretching modes, respectively. The $NH_{2,ads}$ species forms during the final stage of preparation of the H_{ads} layer on the unreconstructed (1×1) surface.[21] A removal of $NH_{2,ads}$ by heating to $T > 400$ K results in the surface reconstruction from the (1×1) surface structure to the (hex) one.

An exposure of the H_{ads} layer to NO results in the disappearance of the bridge state of H_{ads}: the band at 1200 cm^{-1} decreases in an intensity and then disappears (spectra b and c in Figure 1A). The intensities of the characteristic bands of $NH_{2,ads}$, such as $\nu_s(NH_2)$ at 3300 cm^{-1} and $\delta(NH_2)$ at 1450 cm^{-1}, increase, and additionally, a weak band at 825 cm^{-1} and a shoulder at 3400 cm^{-1} become detectable due to wagging [$\omega(NH_2)$] and asymmetric [$\nu_{as}(NH_2)$] modes, respectively.[27] The procedures described above was used thereafter for the preparation of a $NH_{2,ads}$ layer. Since the $NH_{2,ads}$ coverage in the original H_{ads} layer is about 0.01 monolayer (Figure 1A, spectrum a),[21] the maximum attainable $NH_{2,ads}$ coverage is estimated to be 0.12 monolayer after NO exposure of 0.8 langmuir (Figure 1A, spectrum d). The estimation was done assuming a linear dependence of the $\delta(NH_2)$ intensity on θ_{NH_2} and gives a reasonable value for θ_{NH_2} because, according to the stoichiometry of the reaction

$$NO_{ads} + 4H_{ads} \rightarrow H_2O + NH_{2,ads} \qquad (1)$$

the $NH_{2,ads}$ coverage cannot exceed 0.15 monolayer for the initial H_{ads} coverage of 0.6 monolayer.

The amino species starts to disappear after a NO exposure of 1.2 langmuirs that manifests itself in the strong attenuation of the bands attributed to the $NH_{2,ads}$ species (Figure 1A, spectrum e). The consumption of $NH_{2,ads}$ is accompanied by an appreciable increase in nitrogen partial pressure, implying that N_2 is a product of the reaction. After the $NH_{2,ads}$ species is completely consumed, two new bands at 370 and 1585 cm^{-1} appear due to NO adsorbed on the (1×1) surface (Figure 1, spectrum f). The former band is assigned to either a ν(Pt−NO) stretching mode or δ(Pt−N−O) deformation mode,[28] and the latter band is a characteristic of a ν(N−O) stretching vibration.[28] The absence of a band at ca. 1770 cm^{-1}, which characterizes NO adsorbed on structural defects,[23] points to the fact that the (1×1) surface does not reconstruct under the titration of the H_{ads} layer by NO.

To perform an additional characterization of the adsorption layer formed after the H_{ads} titration by NO, TPR spectra of D_2, $^{15}ND_3$, D_2O, $^{15}N_2$, ^{15}NO, O_2, and $^{15}N_2O$ were taken after an exposure of the saturated layer of D_{ads} to NO (3 langmuirs) at 300 K, as shown in Figure 1B. The absence of D-containing species among the desorbing products, excepting a negligible amount of D_2O, supports the conclusion about formation of a NO_{ads} layer. Indeed, the TPR spectra of NO, N_2, O_2, and N_2O are very similar to those observed after NO adsorption on the clean Pt(100)-(1×1) surface.[29]

The reaction between the amino species and NO was studied at 260 K by HREELS (Figure 2A). HREEL spectrum a taken at 100 K from the $ND_{2,ads}$ layer produced as described above (see Figure 1A for details) shows the characteristic modes of $ND_{2,ads}$: $\delta(ND_2)$ scissors at 1085 cm^{-1}, $\nu_s(ND_2)$ symmetric stretching at 2430 cm^{-1}, and poorly resolved $\nu_{as}(ND_2)$ asymmetric stretching at ca. 2530 cm^{-1}. The ν(NO) band at 1585 cm^{-1} reflects the adsorption of a small amount of NO from the background upon cooling. The HREEL spectra b−e in Figure 2A were taken after NO exposure at a partial pressure of 8×10^{-10} mbar and 260 K. A gradual attenuation of the characteristic bands of the $ND_{2,ads}$ species demonstrates the reaction between $ND_{2,ads}$ and impinging NO. As the $ND_{2,ads}$ species is consumed, the N−D stretching band becomes more symmetric and shifts toward higher frequencies by ∼35 cm^{-1}. The ν(NO) band increases in intensity and shifts upward by ∼30 cm^{-1} due to an increase of NO_{ads} coverage.[23,30] The reaction ends with the complete consumption of the amino species at a NO exposure of 1.5 langmuirs. Attempts to perform the reaction at a temperature of 250 K or below failed.

TPR spectra taken after the completion of the reaction between $ND_{2,ads}$ and NO at 260 K exhibits the evolution of only N_2, NO, and O_2 with a minor contribution of N_2O, as shown in

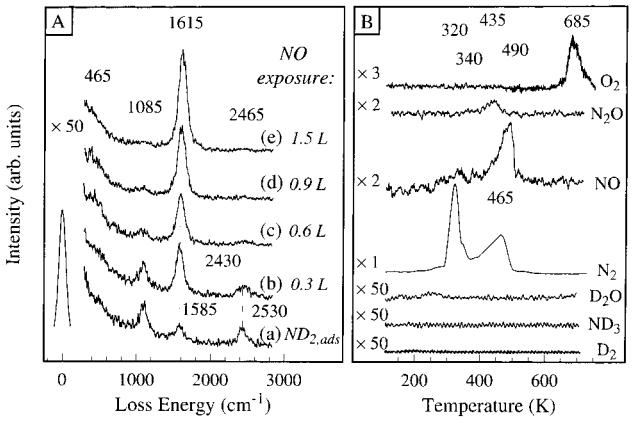

Figure 2. Reaction of the amino species with nitric oxide on the Pt-(100)-(1×1) surface at 260 K. (A) HREEL spectra taken from the $ND_{2,ads}$ layer (a) and after subsequent exposures to (b) 0.3, (c) 0.6, (d) 0.9, and (e) 1.5 langmuirs of NO at 260 K. The procedures of the preparation of the initial $ND_{2,ads}$ layer is described in the text. To prevent the reaction during spectral acquisition, the spectra were recorded at 100 K. (B) TPR spectra of D_2, D_2O, $^{15}ND_3$, $^{15}N_2$, ^{15}NO, O_2, and $^{15}N_2O$ taken after the completion of the reaction between $^{15}ND_{2,ads}$ and ^{15}NO at 260 K (correspond to spectrum e in panel A).

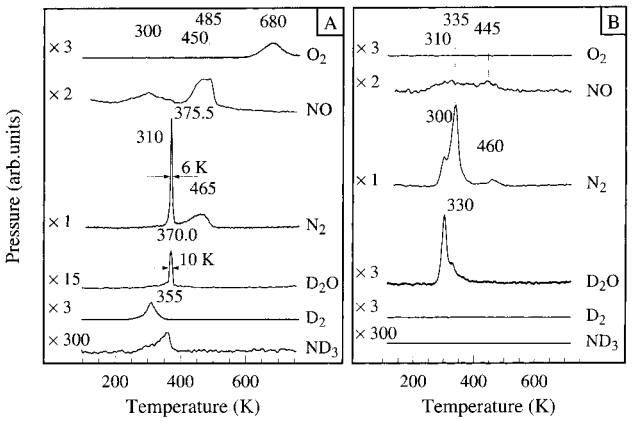

Figure 3. TPR spectra of D_2, $^{15}ND_3$, D_2O, $^{15}N_2$, ^{15}NO, and O_2 taken after an exposure of the $^{15}ND_{2ads}$ layer to (A) 3 langmuirs of ^{15}NO (saturation) and to (B) 0.3 langmuir of ^{15}NO (nonsaturation) at 100 K.

Figure 2B. While the NO, O_2, and N_2O spectra are similar to those observed after NO adsorption on the Pt(100)-(1×1) surface,[29] the N_2 desorption shows an additional low-temperature peak at 320 K along with the traditional peak at 460 K due to the NO_{ads} dissociation. The low-temperature desorption peak of N_2 could be attributed to the recombination of N_{ads} atoms accumulated during the reaction between $ND_{2,ads}$ and NO.

To get additional information on the reaction between the amino species and NO, the TPR were performed in coadsorption layers containing $ND_{2,ads}$ and NO_{ads}. The $ND_{2,ads}$ layer was prepared through the titration of the D_{ads} layer by NO at 300 K; the preparation was controlled by HREELS, as shown in Figure 1A. Since the formation and consumption of amino species are the concurrent processes, the procedures of $ND_{2,ads}$ layer preparation do not allow us to avoid the presence of some amount of D_{ads} in the resulting adsorption layer. NO adsorption over the $ND_{2,ads}$ layer was performed at 100 K. Figure 3 shows two sets of TPR spectra of D_2, D_2O, $^{15}ND_3$, $^{15}N_2$, ^{15}NO, and O_2, which were taken after an exposure of the $ND_{2,ads}$ layer to 3 and 0.3 langmuirs of NO. The NO exposure of 3 langmuirs is sufficient to saturate the surface with adsorbed species, whereas a significant amount of vacant adsorption sites is expected to remain after NO exposure of 0.3 langmuir. In the

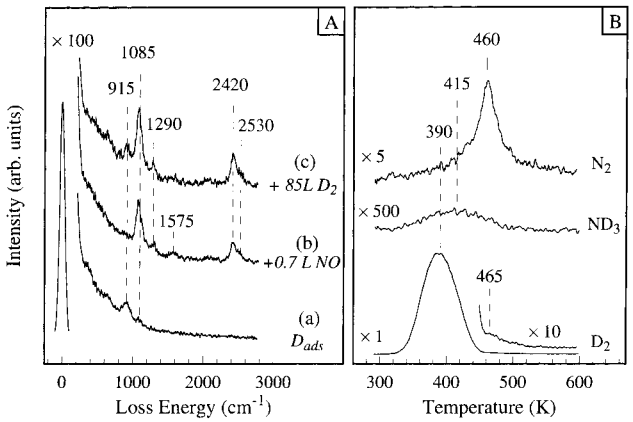

Figure 4. Preparation of the coadsorption layer of the amino species and hydrogen on the Pt(100)-(1×1) surface at 300 K. (A) HREEL spectra taken from (a) the saturated D_{ads} layer, (b) the $ND_{2,ads}$ layer prepared by exposure of the D_{ads} layer to 0.7 langmuir of NO and (c) after subsequent exposure to 85 langmuirs of D_2. (B) TPR spectra of D_2, $^{15}ND_3$, and $^{15}N_2$ taken from the coadsorption layer of $^{15}ND_{2,ads}$ and D_{ads} corresponding to HREEL spectrum c in panel A.

case of the saturated coadsorption layer, TPR exhibits an explosive behavior manifested itself as extremely narrow peaks of D_2O and N_2 at ~370 K with a fwhm of ~5−10 K (Figure 3A). The explosive reaction is initiated by the desorption of D_2 and NO. Ammonia forms during the initiating stage of the reaction as well. As soon as the explosive reaction starts at 355 K, the rate of the ND_3 formation drops down abruptly. $ND_{2,ads}$ and D_{ads} are completely consumed during the explosive reaction, whereas an excess of NO desorbs and dissociates in a similar manner, as was observed for the individual NO_{ads} layers on the Pt(100)-(1×1) surface.[29]

The explosive reaction does not take place for the low NO_{ads} coverage, as shown in Figure 3B. Water and nitrogen evolve as two poorly resolved narrow peaks at ~300 and ~330 K. The presence of sufficient number of vacant sites for NO_{ads} dissociation results in a low reaction temperature, which is slightly below the onset temperature of D_2 desorption and ND_3 formation.

3.2. Reaction between the $NH_{2,ads}$ Species and Hydrogen. The reaction between the $ND_{2,ads}$ species and deuterium was studied in a coadsorption layer of $ND_{2,ads}$ and D_{ads}, prepared as shown in Figure 4A. The $ND_{2,ads}$ layer (spectrum b) was prepared by the titration of the saturated D_{ads} layer (spectrum a) by NO. The HREEL spectrum taken from the $ND_{2,ads}$ layer shows the characteristic modes of $ND_{2,ads}$ species such as $\delta(ND_2)$, $\nu_s(ND_2)$, and $\nu_{as}(ND_2)$. A small contribution of NHD_{ads} results in the appearance of a weak band at 1290 cm^{-1} due to the δ(NHD) mode.[14] A weak band at 1575 cm^{-1} reflects the adsorption of a small amount of NO from the background.[13,23,28,30] An exposure of the $ND_{2,ads}$ layer to 85 langmuirs of D_2 at $P_{D_2} = 1.5 \times 10^{-7}$mbar and 300 K does not lead to any significant changes of the HREEL spectrum, except that the band at 915 cm^{-1} due to the bridge state of D_{ads} re-appears and the ν(NO) band disappears. This means that the $ND_{2,ads}$ species does not convert into ammonia at 300 K even under a great excess of deuterium.

Ammonia formation is observed during TPR in the coadsorption layer of $ND_{2,ads}$ and D_{ads}, as shown in Figure 4B. Along with ammonia desorbing as a broad peak at 415 K, the evolution of N_2 and D_2 is observed. The TPR spectrum of D_2 reveals an intensive peak at 390 K attributed to the recombination of D_{ads}.[21,26,31−34] A weak high-temperature shoulder of the D_2

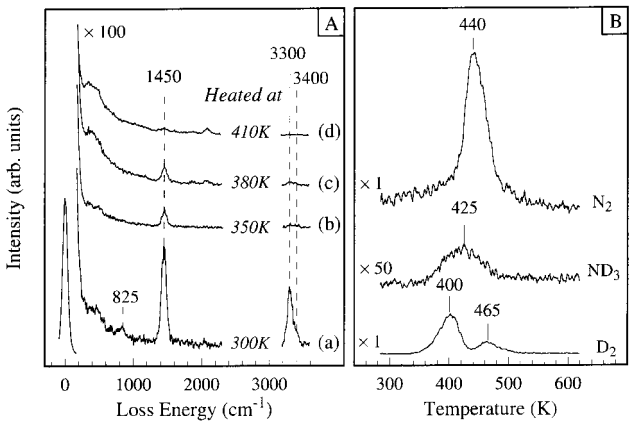

Figure 5. Ammonia formation under the heating of the coadsorption layer containing the amino species and hydrogen on the Pt(100)-(1×1). (A) HREEL spectra taken from (a) the NH_2-H coadsorption layer and after its heating in a stepwise manner in a vacuum for 1 min at (b) 350 K, (c) 380 K, and (d) 410 K. The spectra were recorded at 300 K. (B) TPR spectra of D_2, $^{15}ND_3$, and $^{15}N_2$ taken from the $^{15}ND_2$-D coadsorption layer.

desorption peak at 465 K coincides with N_2 desorption and results from the decomposition of amino species.

The thermal stability of the $NH_{2,ads}$ ($ND_{2,ads}$) species was studied by HREELS and TPR as shown in Figure 5. The $NH_{2,ads}$ species is characterized by the bands due to the $\nu_s(NH_2)$ symmetric and $\nu_{as}(NH_2)$ asymmetric stretchings at 3300 and 3400 cm^{-1}, the $\omega(NH_2)$ wagging at 825 cm^{-1}, and $\delta(NH_2)$ scissors at 1450 cm^{-1}.[14] The heating at 350 K results in a strong attenuation of the $NH_{2,ads}$ bands. It is remarkable that this temperature coincides with the onset temperature of ammonia evolution shown in Figure 5B. Heating at 380 K does not affect the intensity of the $NH_{2,ads}$ characteristic bands (spectrum c in Figure 5A). The $NH_{2,ads}$ species disappears completely after heating at 410 K (spectrum d in Figure 5A). According to the TPR data, the disappearance of the amino species is accompanied by evolution of ND_3, N_2, and D_2 (Figure 5B).

4. Discussion

4.1. Mechanism of the $NH_{2,ads}$ Species Formation and Its Reaction with NO. As mentioned in the Introduction, the NH_{ads} and $NH_{2,ads}$ species were observed during the hydrogenation of adsorbed atomic nitrogen on a number of metal surfaces.[4−12] The formation of $NH_{2,ads}$ species on the Pt(100)-(1×1) surface was reported in ref 14 and in the present work during the reaction between NO and hydrogen at 300 K. The $NH_{2,ads}$ species is supposed to form through the hydrogenation of N_{ads} produced by NO_{ads} dissociation as follows:

$$NO + * \rightarrow NO_{ads} \quad (2a)$$

$$NO_{ads} + * \rightarrow N_{ads} + O_{ads} \quad (2b)$$

$$N_{ads} + H_{ads} \rightarrow NH_{ads} + * \quad (2c)$$

$$NH_{ads} + H_{ads} \rightarrow NH_{2,ads} + * \quad (2d)$$

$$O_{ads} + H_{ads} \rightarrow OH_{ads} + * \quad (2e)$$

$$OH_{ads} + H_{ads} \rightarrow H_2O + 2* \quad (2f)$$

Here symbol * denotes a vacant adsorption site on the surface. O_{ads} formed by NO_{ads} dissociation reacts readily with H_{ads} yielding water,[34,35] which desorbs immediately.[36] The amino species results from the addition of two H_{ads} to N_{ads}. Since the formation of $NH_{2,ads}$ (steps 2c and 2d) competes with the fast production of water (steps 2e and 2f), the amino species can form only in an essential excess of hydrogen in the adsorption layer. As shown in Figure 1A, $NH_{2,ads}$ accumulates during the early stage of the titration as long as the H_{ads} concentration is sufficiently high. As the H_{ads} concentration decreases with increasing NO exposure, the $NH_{2,ads}$ oxidation by NO_{ads} starts to overcome the $NH_{2,ads}$ formation. So, the $NH_{2,ads}$ surface concentration passes through a maximum and then decays to zero.

The amino species can react with NO at temperatures higher than 260 K. $NH_{2,ads}$ is supposed to be oxidized by O_{ads} produced through NO_{ads} dissociation. Since O_{ads} demonstrates a high activity in splitting out hydrogen atoms from molecules such as $NH_{3,ads}$ and $N_2H_{4,ads}$,[37−42] the following mechanism of the reaction between the $NH_{2,ads}$ species and NO_{ads} could be suggested:

$$NO_{ads} + * \rightarrow N_{ads} + O_{ads} \quad (3a)$$

$$NH_{2,ads} + O_{ads} \rightarrow NH_{ads} + OH_{ads} \quad (3b)$$

$$NH_{2,ads} + OH_{ads} \rightarrow NH_{ads} + H_2O + * \quad (3c)$$

$$NH_{ads} + O_{ads} \rightarrow N_{ads} + OH_{ads} \quad (3d)$$

$$NH_{ads} + OH_{ads} \rightarrow N_{ads} + H_2O + * \quad (3e)$$

$$N_{ads} + N_{ads} \rightarrow N_2 + 2* \quad (3f)$$

Reactions 3 include a transient formation of imido species that has an experimental proof. Really, the band at 2430 cm^{-1} possessed by $ND_{2,ads}$ is asymmetric due to unequal contributions of the $\nu_s(ND_2)$ and $\nu_{as}(ND_2)$ modes (Figure 2A, spectrum a), and it becomes more symmetric upon the oxidation of $ND_{2,ads}$ by NO (Figure 2A, spectra b and c). The formation of the imido species characterized by the only ν(ND) stretching mode could explain the symmetrization of this band.

N_{ads} forming in steps 3d and 3e is supposed to recombine, resulting in N_2 evolution (step 3f). Indeed, no evidence was obtained for N_{ads} accumulation during the reaction at 300 K (Figure 1). We have found that N_{ads} producing during titration of NO_{ads} by hydrogen on the Pt(100) surface recombines, yielding N_2 at 300 K.[24] Furthermore, N_{ads} formed during the $NH_{3,ads} + O_{ads}$ reaction on Pt(100) starts to recombine even at ∼200 K.[37] The reason for such an unusually low temperature of N_2 recombinative desorption is supposed to be explained by the destabilizing effect of O_{ads} and NO_{ads} on N_{ads}.[37] The similar effect was reported for Rh(111)[43] and Ru(0001).[44] As demonstrated in the present work, N_{ads} can survive on the Pt(100)-(1×1) surface when the NO + H_2 reaction proceeds at 260 K: the peak of N_2 at 320 K obtained in TPR after the reaction could be assigned to the recombination of N_{ads} (Figure 2B).

As it follows from reactions 3, the vacant adsorption sites play an important role in the reaction between $NH_{2,ads}$ and NO_{ads}; therefore, the variation of the total coverage of adsorbed species changes the character of TPR (Figure 3). TPR in the saturated coadsorption layer demonstrates explosive behavior of N_2 and H_2O formation. The explosive phenomenon was observed previously on the Pt(100) surfaces for the $NO_{ads} + H_{ads}$[45] and $NO_{ads} + CO_{ads}$ reactions.[45−49] According to the mechanism suggested in ref 47, NO_{ads} dissociation is supposed to be the rate-determining step of the surface explosion, so that it is initiated by the releasing of vacant sites necessary for NO_{ads} dissociation. In our case, vacant sites in the saturated ND_2−NO coadsorption layer are released through NO desorption, D_{ads}

recombination, and ND_3 formation (Figure 3A). As soon as the reaction is initiated, the number of vacant sites increases rapidly due to desorption of the products (i.e., N_2 and D_2O), causing an autocatalytic acceleration of the reaction. For the unsaturated coadsorption layer, the surface explosion phenomenon is not observed (Figure 3B) because the number of vacant sites is enough for NO_{ads} dissociation at a much lower temperature before NO and D_2 desorption and ND_3 formation. D_2O is produced in the course of the reaction of O_{ads} with the $ND_{2,ads}$ and D_{ads} species and desorbs as a double peak at 300 and 330 K. N_{ads} is formed by NO_{ads} dissociation and by splitting out of deuterium atoms from $ND_{2,ads}$ at the same temperatures; however, the shapes of TPR spectra of D_2O and N_2 are different. The main portion of D_2O desorbs at 300 K. This reflects the fact that the oxidation of deuterium from $ND_{2,ads}$ and a residual D_{ads} is practically completed at ca. 300 K. N_{ads} formed partially recombines, resulting in the TPR peak at 300 K. However, since the coverage of destabilizing coadsorbates (mainly NO_{ads}) decreases as the reaction proceeds, the major portion of N_{ads} survives on the surface and desorbs at 335 K.

Referring to the low-temperature ammonia evolution shown in Figure 3A, one can propose another route of $NH_{2,ads}$ consumption, namely, via the formation of NH_3 in the $NH_{2,ads} + H_{ads}$ (or $NH_{2,ads} + NH_{2,ads}$) reaction initiated by compression of the $NH_{2,ads} + H_{ads}$ coadsorption layer under NO adsorption. However, the comparison of two sets of TPR spectra presented in panels A and B of Figure 3 evidences that ammonia can be produced only when the total coverage of adsorbed species is close to saturation. Otherwise, the amino species reacts with NO_{ads}, yielding N_2 and H_2O more readily than with H_{ads} (Figure 3B). In the cases when the reaction was monitored by HREELS (Figures 1A and 2A), the total coverage of adsorbed species is far from saturation until the full completion of the reaction, and therefore, ammonia formation is unexpected. Moreover, the formation of NH_3 would lead to the accumulation of some amount of the $NH_{3,ads}$ species on the surface, at least when the reaction is performed at 260 K. However, this is not confirmed by HREELS measurements, showing the absence of a strong characteristic band of the $\delta_s(NH_3)$ umbrella deformation mode in the region of 1150 cm^{-1} (900 cm^{-1} for $ND_{3,ads}$).[38,50]

4.2. Mechanism of the Ammonia Formation. As demonstrated in Figure 4A, the amino species on the Pt(100)-(1×1) surface does not convert into ammonia at 300 K even in a great excess of hydrogen. However, ammonia does form during the heating of the coadsorption layer of the amino species and hydrogen at $T \geq 350$ K (Figures 4B and 5B). The desorption of ammonia is accompanied by the consumption of the $NH_{2,ads}$ species (Figure 5). Likely, the addition of the third hydrogen to the $NH_{2,ads}$ species is the rate-determining step for the ammonia formation from N_{ads} on the Pt(100)-(1×1) surface. The same was established for the N_{ads} hydrogenation on Rh-(111).[6] The following steps for the ammonia formation upon heating could be supposed:

$$NH_{2,ads} + H_{ads} \rightarrow NH_{3,ads} + * \quad (4a)$$

$$NH_{3,ads} \rightarrow NH_3 + * \quad (4b)$$

At $T > 300$ K, the rate of the ammonia desorption is high,[51] therefore, NH_3 evolves into the gas phase immediately after its formation.

One can see in Figures 4B and 5B that the recombination of D_{ads} in the temperature range of 350−400 K competes with the ammonia formation described by steps 4a and 4b. The desorption peak of ammonia is broad and shifted toward higher temperatures from the low-temperature peak of D_2. The broad NH_3 peak might be a superposition of two peaks, which reflects two different processes. Indeed, the N_2 peak and the high-temperature D_2 peak at ∼465 K are likely to result from the decomposition of the $NH_{2,ads}$ species as follows:

$$NH_{2,ads} + 2* \rightarrow N_{ads} + 2H_{ads} \quad (5a)$$

$$N_{ads} + N_{ads} \rightarrow N_2 + 2* \quad (5b)$$

$$H_{ads} + H_{ads} \rightarrow H_2 + 2* \quad (5c)$$

H_{ads} produced in stage 5a can react with the amino species, leading to the formation of ammonia at $T > 400$ K, resulting in broadening of the desorption peak of ammonia. At $T \geq 400$ K all the original H_{ads} leaves the surface via the recombination or ammonia formation (4), therefore, the amino species remains the only source of hydrogen for the further ammonia formation. So, the amino species disproportionates into ammonia and nitrogen.

5. Conclusions

1. The $NH_{2,ads}$ amino species is produced during the titration of the H_{ads} layer with NO on the unreconstructed Pt(100)-(1×1) surface at 300 K. The amino species can readily react with NO at $T \geq 260$ K, yielding water and nitrogen. At a reaction temperature of 260 K, nitrogen can accumulate on the surface as N_{ads}, which recombines and desorbs at $T > 300$ K.

2. TPR in the saturated coadsorption layer of the amino species and NO_{ads} prepared previously at 100 K shows an explosive behavior manifesting itself in the desorption of the reaction products such as N_2 and H_2O as narrow peaks at ∼370 K and with fwhm ∼5−10 K. For the unsaturated layer the reaction starts at a lower temperature by ∼80 K and does not show the explosive behavior.

3. The $NH_{2,ads}$ species plays the role of an intermediate for the ammonia formation. The addition of a hydrogen atom to $NH_{2,ads}$ occurs concurrently with the H_{ads} recombination in the temperature interval of 350−400 K. At temperatures higher than 400 K, amino species disproportionate into N_2 and NH_3.

References and Notes

(1) Shelef, M. *Catal. Rev.—Sci. Eng.* **1975**, *11*, 1.
(2) Bosch, H.; Janssen, F. *Catal. Today* **1987**, *2*, 369.
(3) Taylor, K. *Catal. Rev.—Sci. Eng.* **1993**, *35*, 457.
(4) Tanaka, K.; Yamada, T.; Nieuwenhuys, B. E. *Surf. Sci.* **1991**, *242*, 503.
(5) Yamada, T.; Tanaka, K. *J. Am. Chem. Soc.* **1991**, *113*, 1173.
(6) Van Hardeveld, R. M.; Van Santen, R. A.; Niemantsverdriet, J. W. *J. Phys. Chem. B* **1997**, *101*, 998.
(7) Yamada, T.; Tanaka, K. *J. Am. Chem. Soc.* **1989**, *111*, 6880.
(8) Shi, H.; Jacobi, K.; Ertl, G. *J. Chem. Phys.* **1995**, *102*, 1432.
(9) Dietrich, H.; Jacobi, K.; Ertl, G. *J. Chem. Phys.* **1996**, *105*, 8944.
(10) Dietrich, H.; Jacobi, K.; Ertl, G. *J. Chem. Phys.* **1997**, *106*, 9313.
(11) Takehiro, N.; Mukai, K.; Tanaka, K. *J. Chem. Phys.* **1995**, *103*, 1650.
(12) Yamada, T.; Hirano, H.; Tanaka, K.; Siera, J.; Nieuwenhuys, B. E. *Surf. Sci.* **1990**, *226*, 1.
(13) Zemlyanov, D. Y.; Smirnov, M. Yu.; Gorodetskii, V. V.; Block, J. H. *Surf. Sci.* **1995**, 329, 61.
(14) Zemlyanov, D. Yu.; Smirnov, M. Yu.; Gorodetskii, V. V. *Surf. Sci.* **1997**, *391*, 37.
(15) Slinko, M.; Fink, T.; Löher, T.; Madden, H. H.; Lombardo, S. J.; Imbihl, R.; Ertl, G. *Surf. Sci.* **1992**, *264*, 157.
(16) Makeev, A. G.; Slinko, M. M.; Janssen, N. M. H.; Cobden, P. D.; Nieuwenhuys, B. E. *J. Chem. Phys.* **1996**, *105*, 7210.
(17) Makeev, A. G.; Nieuwenhuys, B. E. *J. Chem. Phys.* **1998**, *108*, 3740. Makeev, A. G.; Nieuwenhuys, B. E. *Surf. Sci.* **1998**, *418*, 432.
(18) Cholach, A. R.; Bulgakov, N. N. *Catal. Lett.* **1997**, *48*, 191. Cholach, A. R.; Bulgakov, N. N. *Catal. Lett.* **1999**, *58*, 183.

(19) Kaichev, V. V.; Sorokin, A. M.; Boronin, V. A.; Badalyan, A. M. *Avtometrija* **1997**, No. 5, 15 (in Russian).
(20) Kaichev, V. V.; Sorokin, A. M.; Badalyan, A. M.; Nikitin, D. Yu.; Moskovkin, O. V. *Instrum. Exp. Tech.* **1997**, *40*, 575.
(21) Zemlyanov, D. Yu.; Smirnov, M. Yu.; Gorodetskii, V. V. *Catal. Lett.* **1997**, *43*, 181.
(22) Bonzel, H. P.; Broden, G.; Pirug, G. *J. Catal*. **1978**, *53*, 96.
(23) Gardner, P.; Tüshaus, M.; Martin, R.; Bradshaw, A. M. *Surf. Sci.* **1990**, *240*, 112.
(24) Zemlyanov, D. Yu.; Smirnov, M. Yu.; Gorodetskii, V. V. *Catal. Lett.* **1994**, *28*, 153.
(25) Zemlyanov, D. Yu.; Smirnov, M. Yu.; Gorodetskii, V. V. *Phys. Low-Dim. Struct.* **1994**, *4/5*, 89.
(26) Klötzer, B.; Bechtold, E. *Surf. Sci*. **1993**, *295*, 374.
(27) The detailed analysis of the characteristic vibrations of $NH_{2,ads}$ as well as $ND_{2,ads}$ and NHD_{ads} was performed elsewhere.[14]
(28) Pirug, G.; Bonzel, H. P.; Hopster, H.; Ibach, H. *J. Chem. Phys.* **1979**, *71*, 593.
(29) Zemlyanov, D. Yu.; Smirnov, M. Yu.; Gorodetskii, V. V. *React. Kinet. Catal. Lett.* **1994**, *53*, 87.
(30) Zemlyanov, D. Yu.; Smirnov, M. Yu. *React. Kinet. Catal. Lett.* **1994**, *53*, 97.
(31) Barteau, M. A.; Ko E. I.; Madix, R. J. *Surf. Sci*. **1981**, *102*, 99.
(32) Pennemann, B.; Olster, K.; Wandelt, K. *Surf. Sci. 1991*, *249*, 35.
(33) Pasteur, A. T.; Dixon-Warren, St. J.; King, D. A. *J. Chem. Phys.* **1995**, *103*, 2251.
(34) Sobyanin, V. A.; Boreskov, G. K.; Cholach, A. R. *Dokl. Akad. Nauk SSSR* **1984**, *278*, 1422 (in Russian).
(35) Helms, C. R.; Bonzel, H. P.; Kelemen, S. J. *Chem. Phys.* **1976**, *65*, 1773.
(36) Ibach, H.; Lehwald, S. *Surf. Sci.* **1980**, *91*, 187; Kizhakevariam, N.; Stuve, E. M. *Surf. Sci.* **1992**, *275*, 223.
(37) Bradley, J. M.; Hopkinson, A.; King, D. A. *J. Phys. Chem.* **1995**, *99*, 17032.
(38) Mieher, W. D.; Ho, W. *Surf. Sci.* **1995**, *322*, 151.
(39) Wagner, M. L.; Schmidt, L. D. *J. Phys. Chem.* **1995**, *99*, 805.
(40) Thornburg, D. M.; Madix, R. J. *Surf. Sci.* **1989**, *230*, 268.
(41) Afsin, B.; Davies, P. R.; Pashuski, A.; Roberts, M. W. *Surf. Sci.* **1991**, *259*, L724.
(42) Afsin, B.; Davies, P. R.; Pashuski, A.; Roberts, M. W.; Vincent, D. *Surf. Sci.* **1993**, *284*, 109.
(43) Root, T. W.; Schmidt, L. D.; Fischer, G. B. *Surf. Sci.* **1983**, *134*, 30.
(44) Hornung, A.; Zemlyanov, D.; Muhler, M.; Ertl, G. Manuscript in preparation.
(45) Lesley, M. V.; Schmidt, L. D. *Surf. Sci*. **1985**, *155*, 215.
(46) Fisher, T. E.; Kelemen, S. R. *J. Catal.* **1978**, *53*, 24.
(47) Fink, Th.; Dath, J.-P.; Basset, M. R. Imbihl, R.; Ertl, G. *Surf. Sci.* **1991**, *245*, 96.
(48) Zagatta, G.; Müller, H.; Wehmeyer, O.; Brandt, M.; Böwering, N.; Heinzmann, U. *Surf. Sci.* **1994**, *307*−*309*, 199.
(49) Zemlyanov, D. Yu.; Smirnov, M. Yu.; Gorodetskii, V. V.; Vovk, E. I. *Catal. Lett.* **1997**, *46*, 201.
(50) Sexton, B. A.; Mitchel, G. E. *Surf. Sci*. **1980**, *99*, 523.
(51) Bradley, J. M.; Hopkinson, A.; King, D. A. *Surf. Sci*. **199**7, *371*, 255.